Available online at www.sciencedirect.com
SCIENCE DIRECT
Tetrahedron
Tetrahedron 62 (2006) 6379–6387

Three different fluorescent responses to transition metal ions using receptors based on 1,2-bis- and 1,2,4,5-tetrakis-(8-hydroxyquinolinoxymethyl)benzene

Prabhpreet Singh and Subodh Kumar*

Department of Chemistry, Guru Nanak Dev University, Amritsar-143005, India

Received 12 December 2005; revised 25 March 2006; accepted 11 April 2006
Available online 8 May 2006

Abstract—The dipod 1,2-bis(8-hydroxyquinolinoxymethyl)benzene (**3**) and tetrapod 1,2,4,5-tetrakis(8-hydroxyquinolinoxymethyl)benzene (**5**) have been synthesized through nucleophilic substitution of respective 1,2-bis(bromomethyl)benzene (**2**) and 1,2,4,5-tetra(bromomethyl)benzene (**4**) with 8-hydroxyquinoline (**1**). For comparison, 1,3,5-tris(8-hydroxyquinolinoxymethyl)benzene derivatives (**7a** and **7b**) have been obtained. The complexation behavior of these podands towards Ag^+, Co^{2+}, Ni^{2+}, Cu^{2+}, Zn^{2+}, and Cd^{2+} metal ions has been investigated in acetonitrile by fluorescence spectroscopy. The sterically crowded 1,2,4,5-tetrapod **5** displays unique fluorescence 'ON–OFF–ON' switching through fluorescence quenching (λ_{max} 395 nm, switch OFF) with <1.0 equiv of Ag^+ and fluorescence enhancement (λ_{max} 495 nm, switch ON) with >3 equiv Ag^+ and can be used for estimation of two different concentrations of Ag^+ at two different wavelengths. The addition of Cu^{2+}, Ni^{2+}, and Co^{2+} metal ions to tetrapod **5** causes fluorescence quenching, i.e., 'ON–OFF' phenomena at λ_{max} 395 nm for <10 μM (1 equiv) of these ions but addition of Zn^{2+} and Cd^{2+} to tetrapod **5** results in fluorescence enhancement with a gradual shift of λ_{em} from 395 to 432 and 418 nm, respectively. Similarly, dipod **3** behaves as an 'ON–OFF–ON' switch with Ag^+, an 'ON–OFF' switch with Cu^{2+}, and an 'OFF–ON' switch with Zn^{2+}. The placement of quinolinoxymethyl groups at the 1,3,5-positions of benzene ring in tripod **7a**–**b** leads to simultaneous fluorescence quenching at λ_{max} 380 nm and enhancement at λ_{max} 490 nm with both Ag^+ and Cu^{2+}. This behavior is in parallel with 8-methoxyquinoline **8**. The rationalization of these results in terms of metal ion coordination and protonation of podands shows that 1,2 placement of quinoline units in tetrapod **5** and dipod **3** causes three different fluorescent responses, i.e., 'ON–OFF–ON', 'ON–OFF', and 'OFF–ON' due to metal ion coordination of different transition metal ions and 1, 3, and 5 placement of three quinolines in tripod **7**, the protonation of quinolines is preferred over metal ion coordination. In general, the greater number of quinoline units coordinated per metal ion in **5** compared with the other podands points to organization of the four quinoline moieties around metal ions in the case of **5**.

1. Introduction

The design and synthesis of target selective receptors with luminescent signaling systems for direct measurement of changes in emission intensities or wavelength, arising due to perturbation upon ion or molecular recognition, have attained a central position in supramolecular chemistry.[1–2]

These recognition phenomena depend primarily on multiple host-guest interactions. Locking of conformations of both the host and the guest make negative contributions to total free energies of the system.[3] So, in addition to the complementarity of binding sites, the correct spatial placement of subunits[4] constitutes a major criterion for designing new receptors.

8-Hydroxyquinoline (oxine) and its derivatives are known to be the best chelaters after EDTA and its derivatives due to their guest modulated chromogenic and fluorescent behavior. Accordingly, they have attained prime significance and have been used in chromatography,[5] detection of metal ions,[6] in organic light emitting diode devices,[7] and in electrochemiluminescence[8] etc. In the case of planar platforms, the contribution of molecular architectures arising due to placement of two or three subunits at 1,3- or 1,3,5-positions on a benzene ring has been well studied in molecular recognition.[9] However, the supramolecular behavior of receptors possessing two or four such functional groups placed symmetrically at 1,2- and 1,2,4,5-positions of a benzene ring has been scarcely studied.[10]

In continuation of our work[11] on syntheses of receptors possessing 8-hydroxyquinoline moieties as the only binding sites, in the present work[12] a fluorescent dipod **3** and a tetrapod **5** possessing two and four 8-hydroxyquinoline units at 1,2- and 1,2,4,5-positions of benzene ring, respectively, have been synthesized and their binding features

* Corresponding author. Fax: +91 183 2258820; e-mail: subodh_gndu@yahoo.co.in

0040–4020/$ - see front matter © 2006 Elsevier Ltd. All rights reserved.
doi:10.1016/j.tet.2006.04.035

towards transition metal ions have been evaluated by fluorescence studies in CH_3CN. For comparison the behavior of 1,3,5-tris(8-hydroxyquinolinoxymethyl)benzene derivatives **7** and 8-methoxyquinoline **8** has been also studied. Dipod **3** and tetrapod **5** show unique switch-like 'ON–OFF–ON' behavior towards Ag^+. Dipod **3** and tetrapod **5** provide three different fluorescent responses to transition metal ions as 'ON–OFF–ON' switch with Ag^+, 'ON–OFF' switch with Cu^{2+}, Co^{2+}, and Ni^{2+} and 'OFF–ON' switch with Zn^{2+} and Cd^{2+}. On moving to 1,3,5-tripods **7** and 8-methoxyquinoline **8** due to preferred protonation over metal ion coordination the occurrence of these phenomena is lowered. To the best of our knowledge, this constitutes the first example of a benzene-based tetrapod organization.

2. Results and discussion

2.1. Synthesis of podands 3, 5, and 7

The nucleophilic substitution of 1,2-bis(bromomethyl)benzene (**2**) with 8-hydroxyquinoline under phase transfer catalyzed conditions provided a white solid. NMR spectroscopy and COSY experiments allowed the spectral assignment. For assigning the signals in the multiplet region, the ^1H NMR spectrum of **3** after addition of 0.1 equiv $AgNO_3$ was recorded (Fig. 1). These spectral data along with ^{13}C NMR spectral data corroborated the structure **3** for this compound.

Similarly, the nucleophilic substitution of 1,2,4,5-tetrakis-(bromomethyl)benzene (**4**) with 8-hydroxyquinoline (**1**) under phase transfer catalyzed conditions provided **5** as a white solid. The positions of all the protons have been assigned by decoupling experiment. These spectral data and ^1H–^1H COSY and ^{13}C NMR spectral data confirmed the structure **5** for this compound. The reactions of tribromides **6a** and **6b** with **1** gave tripods **7a** and **7b**, respectively (Scheme 1).

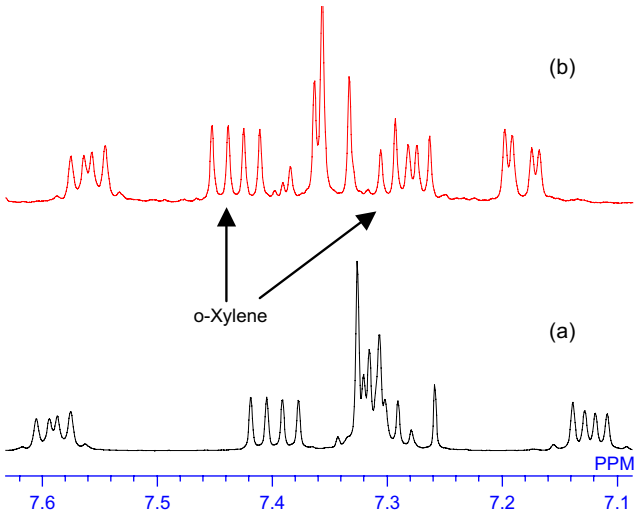

Figure 1. ^1H NMR of (a) dipod **3** (b) dipod **3**+0.1 equiv $AgNO_3$.

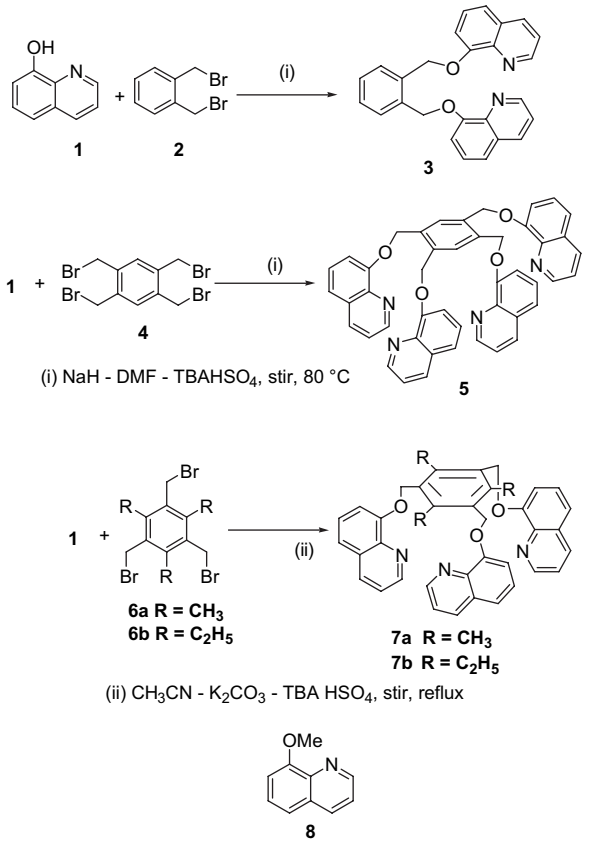

Scheme 1.

2.2. Photophysical behavior of podands 3, 5, 7, and 8 towards transition metal ions

Podands **3**, **5**, **7**, and **8** (10 μM, CH_3CN) in their UV–vis spectra exhibit broad absorption bands at λ_{max} 305 nm due to the 8-alkoxyquinoline moiety. The solutions of podands **3**, **5**, **7**, and **8** on excitation at λ_{max} 305 nm exhibit fluorescence spectra typical of the 8-hydroxyquinoline moieties with λ_{max} at 385 nm, and remain stable within λ_{ex} 305–360 nm. In this work, all the studies have been performed using λ_{ex} 345 nm except in cases when stated otherwise. In the concentration range 1–10 μM, the fluorescence of **3**, **5**, **7**, and **8** is directly proportional to their concentration. This linear increase in fluorescence with concentration indicates that these podands are not susceptible to self quenching and to aggregation processes in this concentration range.

2.2.1. Photophysical behavior of tetrapod 5 towards transition metal ions. In the preliminary investigations, tetrapod **5** (10 μM, CH_3CN) on addition of 50 μM concd of Co^{2+}, Cu^{2+}, and Ni^{2+}, respectively, shows >90% quenching of fluorescence at λ_{max} 385 nm whereas Zn^{2+} and Cd^{2+} ions cause >10 times fluorescence enhancement with a gradual bathochromic shift of λ_{max} from 395 to 432 nm. However on addition of Ag^+, up to 10 μM to tetrapod **5** shows fluorescence quenching at λ_{max} 395 nm and at higher concentration of Ag^+ a delayed emission band appears at λ_{max} 495 nm. Therefore **5** undergoes 'ON–OFF' switching with Co^{2+}, Cu^{2+}, and Ni^{2+} ions, 'OFF–ON' switching with Zn^{2+} and Cd^{2+} and 'ON–OFF–ON' switching with Ag^+.

A solution of tetrapod **5** (10 μM, CH_3CN) on the addition of $AgNO_3$ showed fluorescence quenching, which gradually increased with increasing concentration of $AgNO_3$. A plot of concentration of $AgNO_3$ versus fluorescence at 395 nm showed a linear decrease with up to 15 μM $AgNO_3$ (1.5 equiv) and then a plateau was achieved. On addition of further $AgNO_3$, a new fluorescence band emerged at λ_{max} 495 nm. The fluorescence intensity at 495 nm gradually increased with increased concentration of $AgNO_3$ (Figs. 2–4).

The spectral fitting of the data showed the formation of ML, M_2L, and M_4L complexes with $\log \beta_{ML}=6.8\pm0.2$, $\log \beta_{M_2L}=12.2\pm0.3$, and $\log \beta_{M_4L}=17.3\pm0.6$ (Table 1). Analysis of the distribution of the different species showed that their concentration varied significantly with the concentration of Ag^+. In a 1:1 mixture of **5** and $AgNO_3$, an almost maximum concentration of the 1:1 complex (>75%) is observed. At this concentration nearly 10% of 2:1 $2AgNO_3$ tetrapod **5** is formed. On further increase in the concentration of Ag^+ to 200 μM, the formation of M_2L increases to 97% along with <1% of a 4:1 $4AgNO_3$ tetrapod **5** complex.

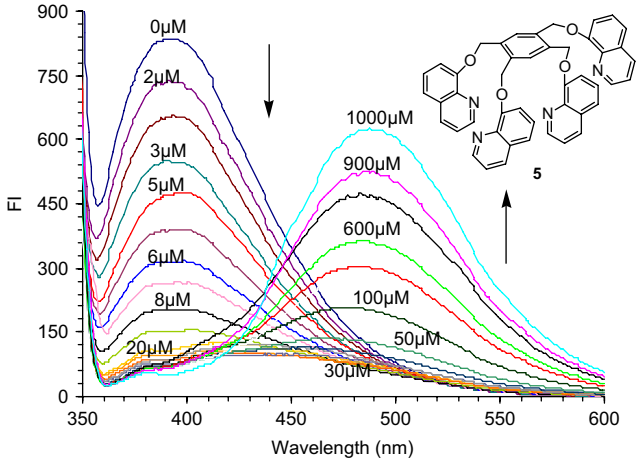

Figure 2. The effect of Ag^+ on the fluorescence spectrum of tetrapod **5** (10 μM).

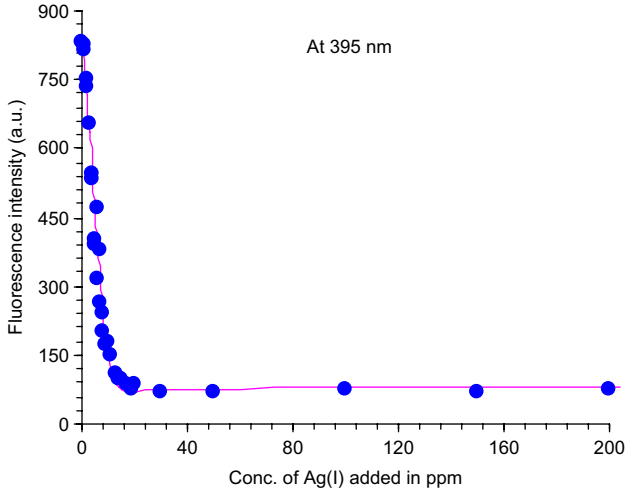

Figure 3. The curve fitting of fluorescence spectral data of **5** at 395 nm on addition of $AgNO_3$. (●) Experimental points, (—) fitted line.

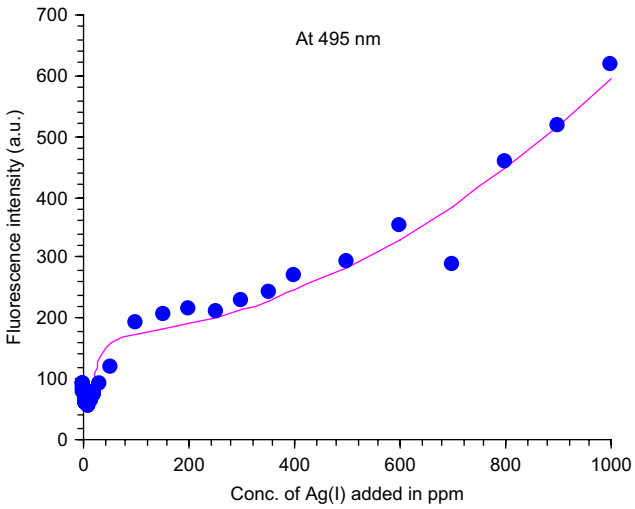

Figure 4. The curve fitting of fluorescence spectral data of **5** (10 μM in CH_3CN) at 495 nm on addition of $AgNO_3$. (●) Experimental points, (—) fitted line.

Even at 1000 μM $AgNO_3$, the 4:1 $4AgNO_3$ tetrapod **5** complex is only formed to 22% extent along with 78% of the 2:1 complex. Due to the existence of number of different stoichiometric complexes of **5** with Ag^+, isosbestic points were not observed (Fig. 5).

The UV–vis spectrum of tetrapod **5** (50 μM, CH_3CN) shows a gradual bathochromic shift from 305 to 314 nm on the addition of 50 μM $AgNO_3$. However, the absorbance between 300–350 nm shows a small (<5%) enhancement in contrast to quenching in fluorescence. Therefore, in tetrapod **5**, the lack of any change in the UV–vis spectrum and 'ON–OFF–ON' switching behavior in fluorescence on addition of $AgNO_3$ point to multiple interactions of Ag^+ with the excited state of **5**.

A solution of tetrapod **5** (10 μM, CH_3CN) on addition of $Cu(NO_3)_2$ showed fluorescence quenching, which gradually increased with increasing concentration of $Cu(NO_3)_2$. On addition of >15 μM $Cu(NO_3)_2$ no further change in fluorescence spectrum was observed. Therefore, in contrast to 'ON–OFF–ON' behavior towards Ag^+, tetrapod **5** with Cu(II) shows 'ON–OFF' behavior. The plot of concentration of $Cu(NO_3)_2$ versus fluorescence at 395 nm shows a linear decrease up to 10 μM $Cu(NO_3)_2$ (1 equiv) and then a plateau is achieved (Fig. 6). The spectral fitting of the data showed the formation of only ML complex with $\log \beta_{ML}=6.6\pm0.1$. In a 1:1 mixture of **5** and $Cu(NO_3)_2$, formation of 1:1 complex (>90%) was observed. Similarly, other paramagnetic ions Co(II) and Ni(II) with **5** showed 'ON–OFF' switch with $\log \beta_{ML}$ value 6.6±0.1 and 5.77±0.06, respectively (Table 1).

Tetrapod **5** on the addition of Zn^{2+} and Cd^{2+} shows fluorescence enhancement. On using λ_{ex} 345 nm, on addition of Zn^{2+} and Cd^{2+} (0.3 equiv) to a solution of **5**, the fluorescence went off scale. So, all studies of Zn^{2+} and Cd^{2+} were performed at λ_{ex} 360 nm. The plot of fluorescence intensity of **5** against concentration of Zn^{2+} shows a gradual fluorescence enhancement using 1–30 μM Zn^{2+} concentration with a gradual red shift of λ_{max} from 385 to 432 nm and between

Table 1. Fluorescence behavior and log β_{MXL} values for podands **5**, **3**, and **7a–b** towards transition metal ions

Serial no.	Metal ion	Fq/Fe[a]	λ_{max} (nm)	log β_{ML_2}	log β_{ML}	log β_{M_2L}	log β_{M_4L}
Tetrapod ***5***							
1	Ag^{+}	'ON–OFF–ON'	$385–385_{fe}–495_{fe}$		6.8±0.2	12.2±0.3	17.3±0.6
2	Cu^{2+}	'ON–OFF'	$385–385_{fq}$		6.6±0.1		
3	Ni^{2+}	'ON–OFF'	$385–385_{fq}$		5.7±0.1		
4	Co^{2+}	'ON–OFF'	$385–385_{fq}$		6.5±0.1		
5	Zn^{2+}	'OFF–ON'	$385–432_{fe}$		5.1±0.1		
6	Cd^{2+}	'OFF–ON'	$385–423_{fe}$		6.6±0.1	11.8±0.5	
Dipod ***3***							
7	Ag^{+}	'ON–OFF–ON'	$385–385_{fe}–495_{fe}$		6.3±0.2	9.5±0.2	
8	Cu^{2+}	'ON–OFF'	$385–385_{fq}$		4.9±0.2		
9	Zn^{2+}	'OFF–ON'	$385–432_{fe}$	14.1±0.4	7.9±0.3		
					log β_{ML}	log β_{M_2L}	log β_{M_3L}
Tripod ***7a***							
10	Ag^{+}	Set on 'OFF-ON'	$385_{fq}–490_{fe}$			11.00±0.06	15.3±0.2
11	Ag^{+}	From UV–vis	$301_{Al}–360_{Ae}$		6.30±0.3	10.50±0.48	15.3±0.3
12	Cu^{2+}	Set on 'OFF–ON'	$385_{fq}–490_{fe}$		5.36±0.7		14.9±0.1
Tripod ***7b***							
13	Ag^{+}	Set on 'OFF–ON'	$385_{fq}–490_{fe}$			10.6±0.1	14.6±0.3
14	Ag^{+}	From UV–vis	$301_{Al}–360_{Ae}$		6.1±0.2	10.6±0.3	15.1±0.3

[a] Fq=fluorescence quenching; Fe=fluorescence enhancement; Al=absorbance lowering; Ae=absorbance enhancement.

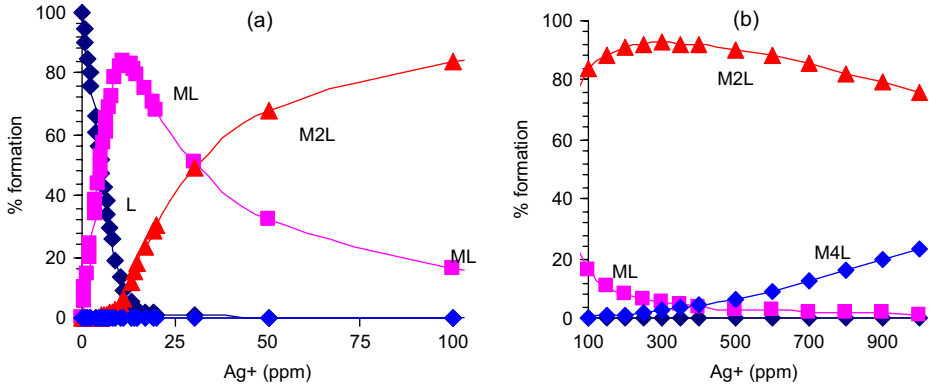

Figure 5. The distribution of ML, M_2L, and M_4L species on addition of $AgNO_3$ to **5** (10 μM in CH_3CN) (a) 0–100 μM $AgNO_3$ (b) 100–1000 μM $AgNO_3$.

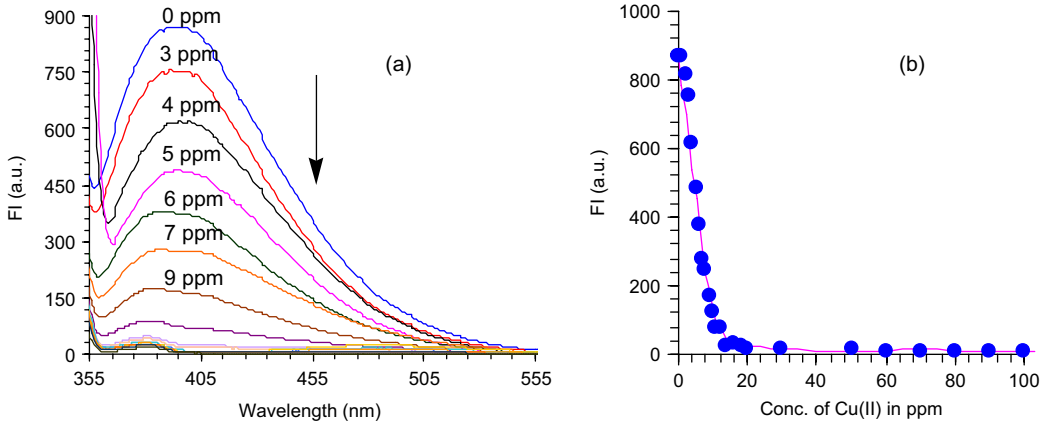

Figure 6. (a) The effect of Cu^{2+} on the fluorescence spectrum of tetrapod **5** in acetonitrile and (b) curve fitting of change in FI of tetrapod **5** (10 μM) at 395 nm on addition of $Cu(NO_3)_2$. (●) Experimental points, (—) fitted line.

30 and 100 μM Zn^{2+}, a plateau is achieved. The spectral fitting of the data showed the formation of ML with log β_{ML}=5.11±0.05. The formation of >80% Zn^{2+}:**5** complex is observed at 50 μM Zn^{2+} (5 equiv).

Similarly, the addition of $Cd(NO_3)_2$ to a solution of **5** caused fluorescence enhancement with a gradual red shift in λ_{max} from 385 to 418 nm (Fig. 7). These data showed the formation of M_2L and ML complexes with log β_{M_2L}=11.83±0.5

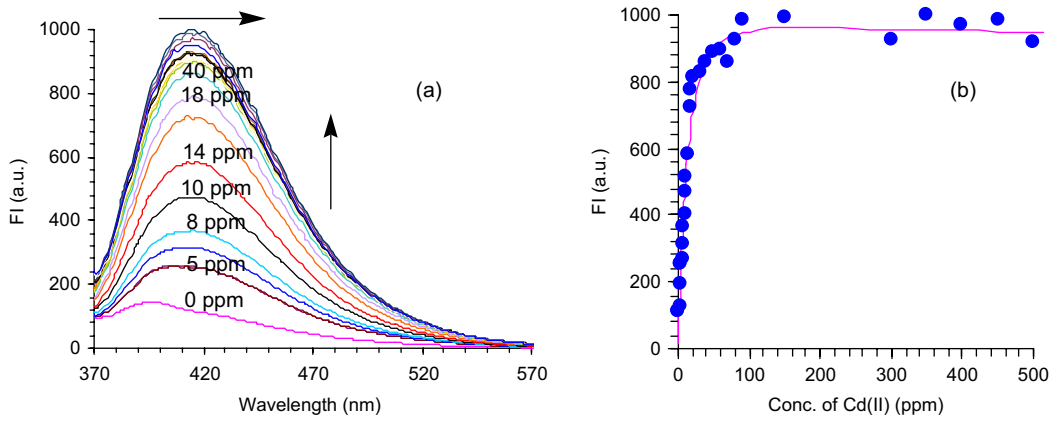

Figure 7. (a) The effect of Cd^{2+} on the fluorescence spectrum of tetrapod **5** and (b) curve fitting of change in FI of tetrapod **5** (10 μM) at 418 nm on addition of $Cd(NO_3)_2$. (●) Experimental points, (—) fitted line.

and log β_{ML}=6.7±0.1. In a 1:2 mixture of **5** and $Cd(NO_3)_2$, an almost maximum concentration of the 1:1 complex (47%) along with small amounts <5% of M_2L was observed. On further increasing the **5**:$Cd(NO_3)_2$ ratio to 1:10, the formation of M_2L increased to nearly 70% along with 30% of ML complex.

2.2.2. Photophysical behavior of dipod 3 towards transition metal ions. A solution of dipod **3** on excitation at λ_{ex} 345 nm showed a gradual decrease in fluorescence on addition of $AgNO_3$, which gradually increased on increasing the concentration of $AgNO_3$.

A plot of concentration of $AgNO_3$ versus fluorescence at 385 nm shows a linear decrease with up to 50 μM $AgNO_3$ (5 equiv) and then a plateau is achieved. During addition of $AgNO_3$, between 10–30 μM (1–3 equiv), no significant change in fluorescence at 395 nm or 500 nm was observed. However, on further addition of $AgNO_3$ a fluorescence band at λ_{max} 500 nm appeared and its intensity gradually increased with an increase in the concentration of $AgNO_3$. The spectral fitting of the titration data of dipod **3** with $AgNO_3$ shows the formation of ML and M_2L complexes with log β_{ML}=6.3±0.2 and log β_{M_2L}=9.5±0.2, respectively (Fig. 8).

Analysis of the distribution of different species showed that their concentration varied significantly with the concentration of Ag^+. In a 1:2 mixture of **3** and $AgNO_3$, an almost nearly maximum concentration of a 1:1 complex (94%) was observed. At this concentration nearly 1% of the 2:1 $2AgNO_3$ dipod **3** was observed. On further increasing the concentration of Ag^+ to 1000 μM, the formation of M_2L increases to 60% along with 40% of the ML complex (Fig. 9).

Dipod **3** (10 μM, CH_3CN) on addition of $Cu(NO_3)_2$ showed fluorescence quenching, which gradually increased with increasing concentration of $Cu(NO_3)_2$. A plot of concentration of $Cu(NO_3)_2$ versus fluorescence at 385 nm shows a fluorescence decrease up to 50 μM and converges for the formation of the ML complex.

Dipod **3**, on addition of $Zn(NO_3)_2$ showed fluorescence enhancement, which goes out of scale at λ_{ex} 343 nm. So, further studies were carried out at λ_{ex} 350 nm. The plot of, fluorescence intensity of **3** against concentration of Zn^{2+} shows gradual fluorescence enhancement from 1 to 50 μM Zn^{2+} concentration with a gradual red shift of the λ_{max} from 385 to 432 nm, and between 50 and 100 μM Zn^{2+} the fluorescence achieved a plateau (Fig. 10). The spectral fitting of the data showed the formation of only ML_2 and ML

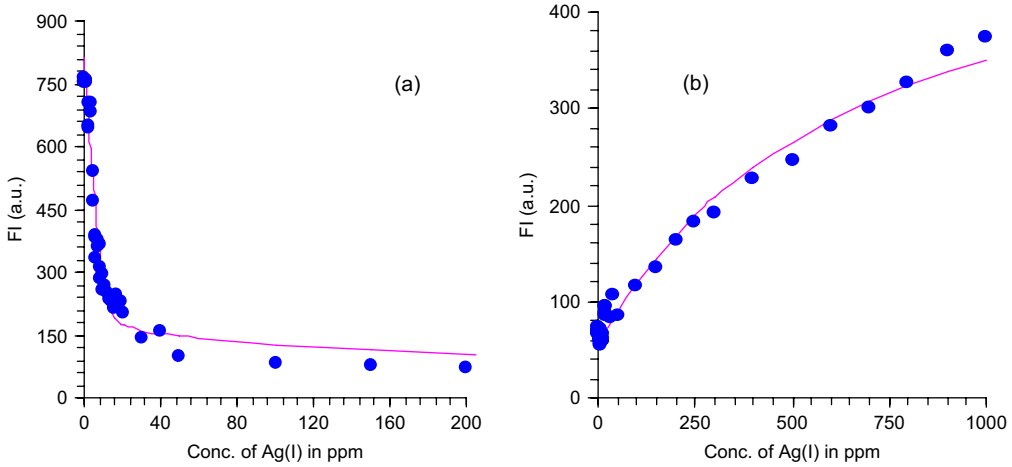

Figure 8. The curve fitting of fluorescence spectral data of **3** on addition of Ag^+: (a) at 385 nm and (b) at 495 nm, respectively. (●) Experimental points, (—) fitted line.

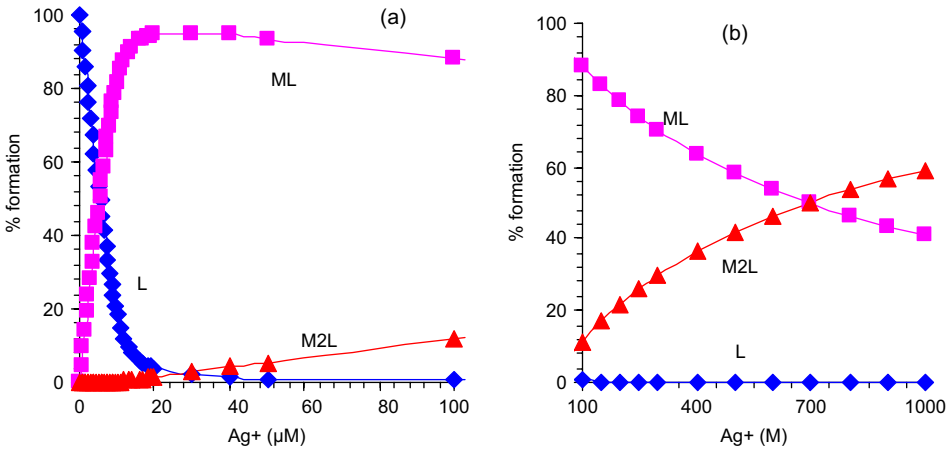

Figure 9. The distribution of ML and M_2L species on addition of $AgNO_3$ to **3** (10 μM in CH_3CN): (a) 0–100 μM $AgNO_3$ (b) 100–1000 μM $AgNO_3$.

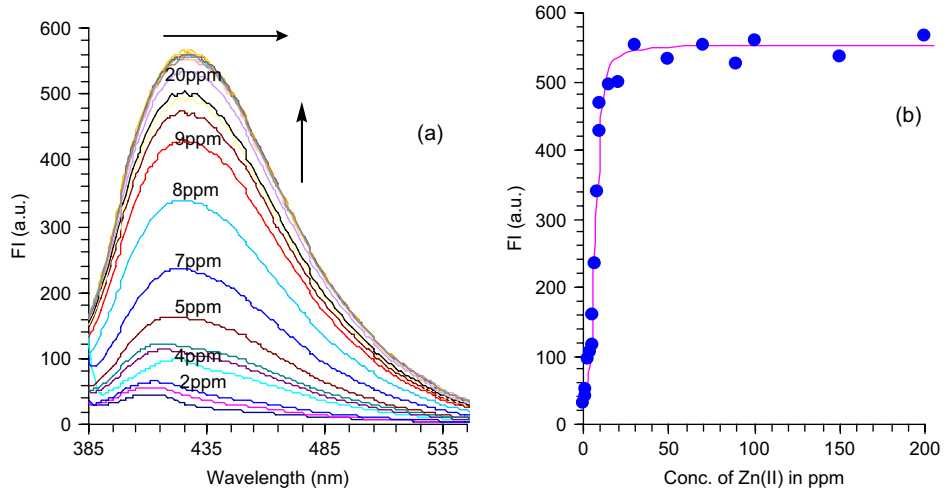

Figure 10. (a) The effect of Zn^{2+} on the fluorescence spectrum of dipod **3** and (b) curve fitting of change in FI of dipod **3** (10 μM) at 428 nm on addition of $Zn(NO_3)_2$. (●) Experimental points, (—) fitted line.

complexes with $\log \beta_{ML_2}=14.10\pm0.48$ and $\log \beta_{ML}=7.9\pm0.3$. In a 1:0.5 mixture of **3** and $Zn(NO_3)_2$, formation of ML_2 complex (>34%) is observed. At this concentration nearly 15% of 1:1 $Zn(NO_3)_2$ dipod **3** is formed. On further increasing the concentration of Zn^{2+} to 50 μM, the formation of ML_2 completely vanishes and 99% ML complex is achieved.

Dipod **3** (10 μM, CH_3CN) in its UV–vis spectrum showed a gradual bathochromic shift from 301 to 315 nm upto addition of 500 μM $AgNO_3$, $Cu(NO_3)_2$, and $Zn(NO_3)_2$. The absorbance between 340 and 360 nm showed small (<5%) enhancement in contrast to >90% fluorescence quenching (with Ag^+ and Cu^{2+}) or >10 times fluorescence enhancement (with Zn^{2+}). Therefore, dipod **3** in parallel with tetrapod **5** on addition of metal ions shows both fluorescence enhancement and fluorescence quenching without any significant change in absorbance in their UV–vis spectra.

2.2.3. Photophysical behavior of tripod 7a–b and 8 towards transition metal ions. Tripods **7a–b** on addition of 100 μM concd of Ag^+ and Cu^{2+}, respectively, showed simultaneous quenching of fluorescence at λ_{max} 380 nm and fluorescence enhancement at λ_{max} 490 nm, and with Zn^{2+} showed erratic behavior both in terms of λ_{max} and fluorescence intensity (FI).

Tripods **7a** and **7b** showed quite similar results and replacement of methyl by ethyl groups on the benzene ring does not have any effect on their metal ion complexation behavior. Tripods **7a–b** (1 μM, CH_3CN) showed fluorescence quenching at 380 nm with simultaneous enhancement at 490 nm on addition of up to 10 μM $AgNO_3$. On further addition of $AgNO_3$ the fluorescence at 380 nm trailed to a small residual value and at 490 nm the emission showed a gradual increase. The fluorescence spectra had two isosbestic points at 431 and 450 nm for both **7a** and **7b** with the formation of M_2L and M_3L complexes (Table 1). In a 1:10 mixture of **7a/7b** and $AgNO_3$ (10 μM), an almost maximum concentration of the M_2L complex (>74%) is observed. At this concentration nearly 13% of M_3L is formed. On further increasing the concentration of $AgNO_3$ to 100 μM, the formation of M_3L increases to 67% along with 33% of M_2L complex.

The UV–vis spectrum of tripod **7a/7b** (10 μM, CH_3CN) showed a simultaneous decrease in absorbance at λ_{max}

301 nm and an increase in the absorbance at λ_{max} 360 nm on gradual addition of $AgNO_3$ between 1 and 1000 μM (Fig. 11). All the spectral lines passed through an isosbestic point at 334 nm. These data converge to the formation of ML, M_2L, and M_3L complexes (Table 1). The similar stability constants arising from both UV–vis and fluorescence spectra data (Table 1, entries 10, 11, 13, and 14) confirm their concomitant presence.

Similarly, addition of $Cu(NO_3)_2$ to **7a/7b** showed simultaneous fluorescence quenching at λ_{max} 380 nm and enhancement at λ_{max} 490 nm with two isosbestic points at 431 and 450 nm and converged to the formation of only ML and M_3L complexes (Table 1). In a 1:10 mixture of **7a** and $Cu(NO_3)_2$, the formation of ML (58%) and M_3L complexes (16%) was observed and at 100 μM Cu^{2+} only formation of M_3L was observed.

Characteristically, like tripods **7a/7b**, 8-methoxyquinoline **8** with both $AgNO_3$ and $Cu(NO_3)_2$ showed simultaneous fluorescence quenching at λ_{max} 395 nm and enhancement at λ_{max} 500 nm due to the formation of ML complex with $\log \beta_{ML}=5.2\pm0.05$. Also, like tripods **7**, UV–vis spectrum of 8-methoxyquinoline **8** on gradual addition of $AgNO_3$ or $Cu(NO_3)_2$ showed simultaneous decrease in absorbance at λ_{max} 301 nm and increase in absorbance at λ_{max} 360 nm.

Therefore, podands **3** and **5**, where quinoline units are placed at adjacent carbons of benzene ring, show differential fluorescence phenomena with transition metal ions without any significant change in their UV–vis spectra but, tripods **7a/7b** and 8-methoxyquinoline **8**, exhibit a fluorescence change, which is parallel to the change in their UV–vis spectra.

A plot of the number of quinoline units/Ag^+ cation versus concentration of Ag^+ shows that both dipod **3** and tetrapod **5** organize higher numbers of quinoline units around Ag^+ than in the case of 8-methoxyquinoline **8** and tripod **7** (Fig. 12). At less than 5 equiv of $AgNO_3$, the tetrapod **5** shows significantly higher numbers of quinoline units around Ag^+ than in the case of **3**, which in turn shows a higher number of quinolines per Ag^+ than in the cases of **7** and **8**.

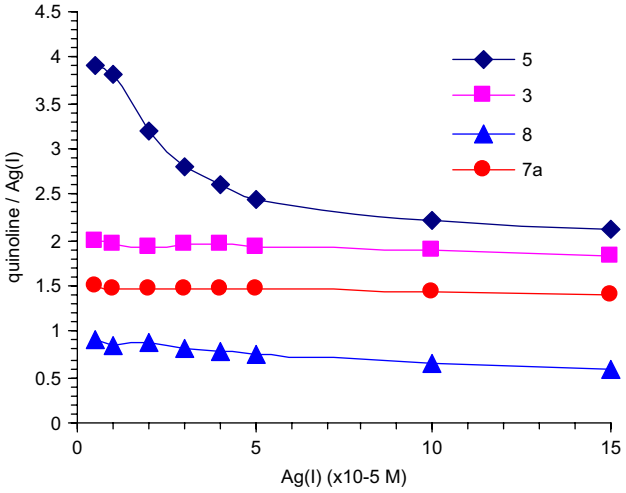

Figure 12. The plot of number of quinoline units per Ag^+ in podands **3**, **5**, **7**, and **8**.

The formation of only ML complexes by **5** with other transition metal ions further exhibits the organization of four quinoline moieties around each metal ion. All these results clearly point to the organization of four quinoline units around metal ions in the case of **5**.

In order to rationalize if some of these metal ion induced fluorescence phenomenon arise due to protonation[13] of the quinoline moieties, the podands **3**, **5**, **7a**, and **8** were titrated against perchloric acid. It is found that in case of dipod **3** and tetrapod **5**, the protonation with $HClO_4$ has much stronger effect on 'ON–OFF–ON' phenomenon. Therefore, dipod **3** and tetrapod **5** on addition of metal ions show change in fluorescence due to metal ion coordination. However, in case of tripods **7a** and **7b** and monopod **8**, the changes in fluorescence behavior on addition of metal ions are in parallel with protonation and could be due to metal salt mediated protonation of tripod **7** and monopod **8**.

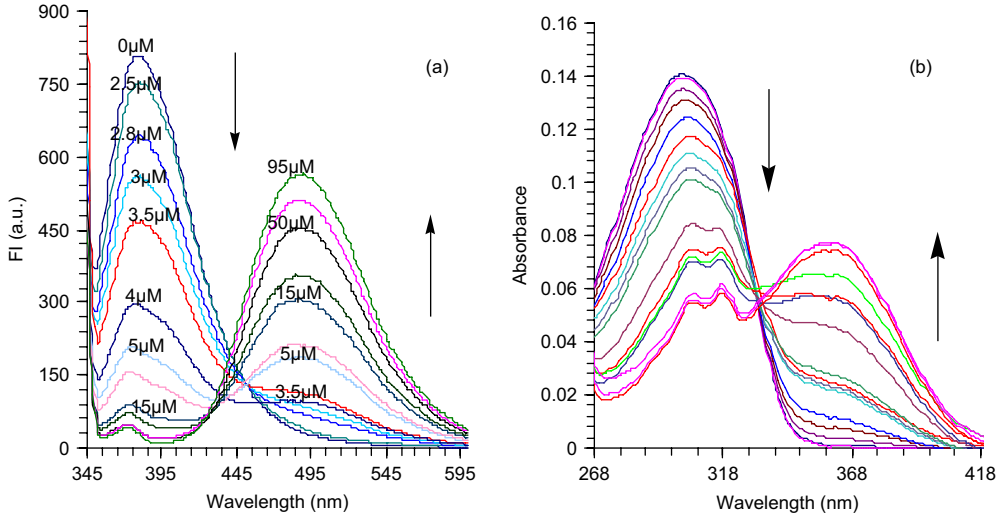

Figure 11. The effect of Ag^+ on: (a) fluorescence spectrum and (b) UV–vis spectrum of **7a**.

3. Experimental

3.1. General details

Melting points were determined in capillaries and are uncorrected. ^{1}H NMR spectra were recorded on JEOL Al 300 MHz instrument using $CDCl_3$ solution containing tetramethylsilane as an internal standard. The chemical shifts are reported in δ values relative to TMS and coupling constants (J) are expressed in hertz. ^{13}C NMR spectra were recorded at 75 MHz and values are reported relative to $CDCl_3$ signal at δ 77.0. Chromatography was performed with silica gel 100–200 mesh and the reactions were monitored by thin layer chromatography (TLC) with glass plates coated with silica gel HF-254. 1,2-Bis(bromomethyl)benzene[14] (**2**), 1,2,4,5-tetrakis(bromomethyl)benzene[15] (**4**), 1,3,5-trimethyl-2,4,6-tris(bromomethyl)benzene[16] (**6a**), 1,3,5-triethyl-2,4,6-tris(bromomethyl)benzene[17] (**6b**), and 8-methoxyquinoline[18] were synthesized according to reported procedures.

3.1.1. 1,2-Bis(8-hydroxyquinolinoxymethyl)benzene (3). A solution of 8-hydroxyquinoline (1.38 g, 9.5 mmol), NaH (pre-washed with hexane) (380 mg, 15.8 mmol), and tetrabutylammonium hydrogen sulfate (20 mg) (catalyst) in DMF (30 ml) was stirred at 80 °C. After 30 min, 1,2-bis(bromomethyl)benzene (**2**) (1.00 g, 3.8 mmol) was added and stirring was continued at 80 °C. After completion of the reaction (tlc, 24 h), the solid residue was filtered off and was washed with ethyl acetate. The combined filtrate was evaporated under vacuum and the solid residue was purified by column chromatography over silica gel (60–120 mesh) using a mixture of CH_2Cl_2/ethyl acetate/MeOH (80:17:3, v/v) to obtain pure **5**, 716 mg, 48%, white solid, mp 112–115 °C (CH_3CN), FAB mass m/z 392 (M^++H); ^{1}H NMR ($CDCl_3$) (300 MHz): δ 5.62 (s, 2×OCH_2, 4H), 7.12 (dd, J_1=5.8 Hz, J_2=3.0 Hz, 2H, ArH), 7.28–7.34 (m, 6H, 2×HQ-H6, 5, 7), 7.40 (dd, J_1=8.4 Hz, J_2=3.9 Hz, 2H, 2×HQ-H3), 7.59 (dd, J_1=5.7 Hz, J_2=3.3 Hz, 2H, ArH), 8.09 (dd, J_1=8.4 Hz, J_2=1.8 Hz, 2H, 2×HQ-H4), 8.92 (dd, J_1=4.2 Hz, J_2=1.8 Hz, 2H, 2×HQ-H2); ^{13}C NMR ($CDCl_3$) (75 MHz) (normal/DEPT-135): δ 69.1 (−ve, CH_2), 110.0 (+ve, ArCH), 119.8 (+ve, ArCH), 121.5 (+ve, ArCH), 126.5 (+ve, ArCH), 128.2 (+ve, ArCH), 128.7 (+ve, ArCH), 129.4 (ab, ArC), 134.9 (ab, ArC), 135.7 (+ve, ArCH), 140.5 (ab, ArC), 149.2 (+ve, ArCH), 154.2 (ab, ArC). Found C, 79.3; H, 5.4; N, 6.9%. $C_{26}H_{20}N_2O_2$ requires C, 79.57; H, 5.14; N, 7.14%.

3.1.2. 1,2,4,5-Tetrakis(8-hydroxyquinolinoxymethyl)-benzene (5). The reaction of 8-hydroxyquinoline with 1,2,4,5-tetrakis(bromomethyl)benzene (**4**) using the above procedure provided **5**, 633 mg, 40%, white solid, mp 233–237 °C (CH_3CN/$CHCl_3$), FAB mass m/z 707 (M^++H); ^{1}H NMR ($CDCl_3$) (300 MHz): δ 5.62 (s, 4×CH_2, 8H), 7.00 (d, J=7.2 Hz, 4H, 4×HQ-H7), 7.19–7.30 (m, 8H, 4×HQ-H6, 5), 7.37 (dd, J_1=8.1 Hz, J_2=4.2 Hz, 4H, 4×HQ-H3), 7.80 (s, 2H, ArH), 8.06 (d, J=6.9 Hz, 4H, 4×HQ-H4), 8.86 (d, J=2.7 Hz, 4H, 4×HQ-H2); ^{13}C NMR ($CDCl_3$/DMSO-d_6) (75 MHz) (normal/DEPT-135): δ 67.36 (−ve, CH_2), 112.5 (+ve, ArCH), 119.0 (+ve, ArCH), 119.1 (ab, ArC), 121.1 (+ve, ArCH), 128.2 (ab, ArC), 128.3 (+ve, ArCH), 128.5 (+ve, ArCH), 133.4 (ab, ArC), 143.2 (+ve, ArCH), 144.5 (+ve, ArCH), 147.2 (ab, ArC). Found C, 77.93; H, 4.7; N, 7.9%. $C_{46}H_{34}N_4O_4$ requires C, 78.17; H, 4.85; N, 7.93%.

3.1.3. 1,3,5-Tris(8-hydroxyquinolinoxymethyl)-2,4,6-trimethylbenzene (7a). The solution of 2,4,6-trimethyl-1,3,5-tris(bromomethyl)benzene (**6a**) (1.00 g, 2.5 mmol), K_2CO_3 (1.03 g, 7.5 mmol), 8-hydroxyquinoline (1.08 g, 7.5 mmol), and TBA·HSO_4 (20 mg) in acetonitrile (30 ml) was refluxed with stirring for 10 h. The solvent was distilled off. The crude mixture was diluted with water and was extracted with ethyl acetate. The organic layer was dried over Na_2SO_4 and solvent was distilled off. The residue was column chromatographed over silica gel column to isolate **7a**, 430 mg, 34%, white solid, mp 200–202 °C (acetonitrile), FAB mass m/z 592 (M+H); ^{1}H NMR ($CDCl_3$): δ 2.51 (s, 9H, 3×CH_3), 5.33 (s, 6H, 3×CH_3), 7.21 (d, 3H, J_1=8 Hz, J_2=2 Hz, 3×HQ-H7), 7.32–7.49 (m, 9H, 3×HQ-H3, 5, 6), 8.08 (dd, 3H, J_1=10 Hz, J_2=4 Hz, 2×HQ-H4), 8.88 (dd, 3H, J_1=8 Hz, J_2=4 Hz, 3×HQ-H2); ^{13}C NMR ($CDCl_3$): δ 16.38 (+ve, CH_3), 66.72 (−ve, OCH_2), 109.96 (+ve, CH), 120.05 (+ve, CH), 121.59 (+ve, CH), 126.73 (+ve, CH), 129.56 (ab, C), 131.48 (ab, C), 135.69 (+ve, CH), 140.04 (ab, C), 140.67 (ab, C), 149.29 (+ve, CH), 155.20 (ab, C). Found C, 79.2; H, 5.6; N, 7.1%. $C_{39}H_{33}N_3O_3$ requires C, 79.19; H, 5.58; N, 7.12%.

3.1.4. 1,3,5-Tris(8-hydroxyquinolinoxymethyl)-2,4,6-triethylbenzene (7b). The reaction of **6b** with 8-hyroxyquinoline (**1**) by the above procedure gave **7b**, 440 mg, 30%, thick transparent liquid, FAB mass 634 [M+H]; ^{1}H NMR ($CDCl_3$): δ 1.29 (t, J=7.2 Hz, 9H, 3×CH_3), 2.96 (q, J=7.2 Hz, 6H, 3×CH_2), 5.35 (s, 6H, 3×OCH_2), 7.31 (dd, J_1=7.5 Hz, J_2=1.2 Hz, 3H, 3×HQ-H7), 7.35–7.54 (m, 9H, 3×HQ-H3, 5, 6), 8.13 (dd, 3H, J_1=8.4 Hz, J_2=1.8 Hz, 3H, 3×HQ-H4), 8.91 (dd, J_1=4.2 Hz, J_2=1.8 Hz, 3H, 3×HQ-H2); ^{13}C NMR ($CDCl_3$): δ 16.57 (+ve, CH_3), 23.37 (−ve, CH_2), 65.71 (−ve, OCH_2), 109.72 (+ve, CH), 119.99 (+ve, CH), 121.56 (+ve, CH), 126.70 (+ve, CH), 129.55 (ab, C), 130.69 (ab, C), 135.87 (+ve, CH), 140.52 (ab, C), 146.88 (ab, C), 149.02 (+ve, CH), 155.22 (ab, C). Found C, 79.54; H, 6.15; N, 7.1%. $C_{39}H_{33}N_3O_3$ requires C, 79.59; H, 6.20; N, 7.08%.

3.1.5. UV–vis and fluorescence experiments. UV–vis absorption and fluorescence spectra were recorded on Shimadazu UV-1601-PC spectrophotometer and Shimadazu RF1501 spectrofluorophotometer with a 1 cm quartz cell at 25±0.1 °C. The solutions of **3**, **5**, **7a**, and **8** and metal nitrates were prepared in double distilled acetonitrile. The number of solutions containing **3/5/7a/8** (10 μM) and different concentrations of metal nitrates were prepared and were kept at 25±1 °C for 2 h before recording their absorption or fluorescence spectra. The spectra obtained were analyzed through curve fitting procedures by using SPECFIT 3.0.36 to determine the stability constants and the distribution of various species.

Acknowledgements

We thank UGC, New Delhi for SAP program; DST, New Delhi for financial assistance and FIST program and CDRI, Lucknow for CHN and mass spectral data.

References and notes

1. (a) de Silva, A. P.; Gunaratne, H. Q. N.; Gunnlaugsson, T.; Huxley, A. J. M.; McCoy, C. P.; Rademacher, J. T.; Rice, T. E. *Chem. Rev.* **1997**, *97*, 1515–1566; (b) Rurack, K.; Resch-Genger, U. *Chem. Soc. Rev.* **2002**, *31*, 116–127; (c) DeSilva, A. P.; Fox, D. B.; Huxley, A. J. M.; McClenaghan, N. D.; Roiran, J. *Coord. Chem. Rev.* **1999**, *186*, 297–306; (d) Lavigne, J. J.; Anslyn, E. V. *Angew. Chem., Int. Ed.* **2001**, *40*, 3118–3130; (e) Fabrizzi, L.; Licchelli, M.; Rabaioli, G.; Taglietti, A. F. *Coord. Chem. Rev.* **2000**, *205*, 85–108; (f) de Silva, A. P.; Fox, D. B.; Huxley, A. J. M.; Moody, T. S. *Coord. Chem. Rev.* **2000**, *205*, 41–57; (g) Amendola, V.; Fabrizzi, L.; Licchelli, M.; Mangano, C.; Pallavicini, P.; Parodi, L.; Poggi, A. *Coord. Chem. Rev.* **1999**, *190–192*, 649–669.
2. (a) Gunnlaugsson, T.; Lee, T. C.; Parkesh, R. *Org. Biomol. Chem.* **2003**, *1*, 3265–3267; (b) Guo, X.; Qian, X.; Jia, L. *J. Am. Chem. Soc.* **2004**, *126*, 2272–2273; (c) Resendiz, M. J. E.; Noveron, J. C.; Disteldorf, H.; Fischer, S.; Stang, P. J. *Org. Lett.* **2004**, *6*, 651–653; (d) Arimori, S.; Phillips, M. D.; James, T. D. *Tetrahedron Lett.* **2004**, *45*, 1539–1542; (e) Gao, X.; Zhang, Y.; Wang, B. *Org. Lett.* **2003**, *5*, 4615–4618; (f) Kang, J.; Choi, M.; Kwon, J. Y.; Lee, E. Y.; Yoon, J. *J. Org. Chem.* **2002**, *67*, 4384–4386; (g) Moon, S. Y.; Cha, N. R.; Kim, Y. H.; Chang, S.-K. *J. Org. Chem.* **2004**, *69*, 181–183; (h) Bu, J.-H.; Zheng, Q.-Y.; Chen, C.-F.; Huang, Z.-T. *Org. Lett.* **2004**, *6*, 3301–3303; (i) Tumambac, G. E.; Rosencrance, C. M.; Wolf, C. *Tetrahedron* **2004**, *60*, 11293–11297.
3. (a) Williams, D. H.; Westwell, M. S. *Chem. Soc. Rev.* **1998**, *27*, 57–63; (b) Peterson, B. R.; Wallimann, P.; Carcanague, D. R.; Diederich, F. *Tetrahedron* **1995**, *51*, 401–421; (c) Searle, M. S.; Westwell, M. S.; Williams, D. H. *J. Chem. Soc., Perkin Trans. 2* **1995**, 141–151.
4. (a) Cram, D. J. *Angew. Chem., Int. Ed. Engl.* **1986**, *25*, 1039–1057; (b) Cram, D. J. *Angew. Chem., Int. Ed. Engl.* **1988**, *27*, 1009–1020.
5. (a) Saroka, K.; Vithanage, R. S.; Phillips, D. A.; Walker, B.; Dasgupta, P. K. *Anal. Chem.* **1987**, *59*, 629–636; (b) Marshall, M. A.; Mottola, H. A. *Anal. Chem.* **1985**, *57*, 375–376; (c) Lucy, C. A.; Liwen, Y. *J. Chromatogr., A* **1994**, *671*, 121–129; (d) De Armas, G.; Miro, M.; Cladera, A.; Estela, J. M.; Cerda, V. *Anal. Chim. Acta* **2002**, *455*, 149–157.
6. (a) Bronson, R. T.; Montalti, M.; Prodi, L.; Zaccheroni, N.; Lamb, R. D.; Dalley, N. K.; Izatt, R. M.; Bradshaw, J. S.; Savage, P. B. *Tetrahedron* **2004**, *60*, 11139–11144; (b) Youk, J.-S.; Kim, Y. H.; Kim, E.-J.; Youn, N. J.; Chang, S.-K. *Bull. Korean Chem. Soc.* **2004**, *25*, 869–872; (c) Bronson, R. T.; Bradshaw, J. S.; Savage, P. B.; Fuangswasdi, S.; Lee, S. C.; Krakowiak, K. E.; Izatt, R. M. *J. Org. Chem.* **2001**, *66*, 4752–4758; (d) Kawakami, J.; Bronson, R. T.; Xue, G.; Bradshaw, J. S.; Izatt, R. M.; Savage, P. B. *Supramol. Chem.* **2001**, *1*, 221–227; (e) Xue, G.; Bradshaw, J. S.; Dalley, N. K.; Savage, P. B.; Krakowiak, K. E.; Izatt, R. M.; Prodi, L.; Montalti, M.; Zaccheroni, N. *Tetrahedron* **2001**, *57*, 7623–7628; (f) Xue, G.; Bradshaw, J. S.; Song, H.; Bronson, R. T.; Savage, P. B.; Krakowiak, K. E.; Izatt, R. M.; Prodi, L.; Montalti, M.; Zaccheroni, N. *Tetrahedron* **2001**, *57*, 87–91; (g) Bordunov, A. V.; Bradshaw, J. S.; Zhang, X. X.; Dalley, N. K.; Kou, X.; Izatt, R. M. *Inorg. Chem.* **1996**, *35*, 7229–7240; (h) Zhang, X. X.; Bordunov, A. V.; Bradshaw, J. S.; Dalley, N. K.; Kou, X.; Izatt, R. M. *J. Am. Chem. Soc.* **1995**, *117*, 11507–11511.
7. (a) Wang, S. *Coord. Chem. Rev.* **2001**, *215*, 79–98; (b) Chen, C. H.; Shi, J. *Coord. Chem. Rev.* **1998**, *171*, 161–174.
8. (a) Gross, E. M.; Anderson, J. D.; Slaterbeck, A. F.; Thayumanavan, S.; Barlow, S.; Zhang, Y.; Marder, S. R.; Hall, H. K.; Flore, N. M.; Wang, J.-F.; Mash, E. A.; Armstrong, N. R.; Wightman, R. M. *J. Am. Chem. Soc.* **2000**, *122*, 4972–4979; (b) Muegge, B. D.; Brooks, S.; Richter, M. M. *Anal. Chem.* **2003**, *75*, 1102–1105.
9. For a benzene-based tripodal receptor for cations and anions see selected examples (a) Walsdorff, C.; Saak, W.; Pohl, S. *J. Chem. Soc., Dalton Trans.* **1997**, 1857–1861; (b) Ahn, K. H.; Ku, H.-Y.; Kim, Y.; Kim, S.-G.; Kim, Y. K.; Son, H. S.; Ku, J. K. *Org. Lett.* **2003**, *5*, 1419–1422; (c) Nguyen, B. T.; Wiskur, S. L.; Anslyn, E. V. *Org. Lett.* **2004**, *6*, 2499–2501; (d) Simaan, S.; Siegel, J. S.; Biali, S. E. *J. Org. Chem.* **2003**, *68*, 3699–3701; (e) Seong, H. R.; Kim, D.-S.; Kim, S.-G.; Choi, H.-J.; Ahn, K. H. *Tetrahedron Lett.* **2004**, *45*, 723–727; (f) Amendola, V.; Fabbrizzi, L.; Monzani, E. *Chem.—Eur. J.* **2004**, *10*, 76–82; (g) Abe, H.; Aoyagi, Y.; Inouye, M. *Org. Lett.* **2005**, *7*, 59–61; (h) Kim, T. W.; Yoon, H. Y.; Park, J.-H.; Kwon, O.-H.; Jang, D.-J.; Hong, J.-I. *Org. Lett.* **2005**, *7*, 111–114.
10. For 1,2,4,5-tetrakis(phenylethynyl)benzene systems see selected examples (a) Marsden, J. A.; Miller, J. J.; Haley, M. M. *Angew. Chem., Int. Ed.* **2004**, *43*, 1694–1697; (b) Iyoda, M.; Sirinintasak, S.; NishiYama, Y.; Vorasingha, A.; Sultana, F.; Nakao, K.; Kuwatani, Y.; Matsuyama, H.; Yoshida, M.; Miyake, Y. *Synthesis* **2004**, 1527–1531; (c) Kondo, K.; Yasuda, S.; Sakaguchi, T.; Miya, M. *J. Chem. Soc., Chem. Commun.* **1995**, 55–56.
11. Kumar, S.; Kaur, S.; Singh, G. *Supramol. Chem.* **2003**, *15*, 65–67.
12. Preliminary communication. Singh, P.; Kumar, S. *Tetrahedron Lett.* **2006**, *47*, 109–112.
13. Beer, P. D.; Smith, D. K. *J. Chem. Soc., Dalton Trans.* **1998**, 417–423.
14. Wilhelm, W. *J. Org. Chem.* **1952**, *17*, 523–528.
15. Stapler, J. T.; Bornstein, J. *J. Heterocycl. Chem.* **1973**, *10*, 983–988.
16. Van der Made, A. W.; Van der Made, R. H. *J. Org. Chem.* **1993**, *58*, 1262–1263.
17. Cabell, L. A.; Best, M. D.; Lavigne, J. J.; Schneider, S. E.; Perreault, M. D.; Monahan, M.-K.; Anslyn, E. V. *J. Chem. Soc., Perkin Trans. 2* **2001**, 315–323.
18. Jain, V. K.; Mason, J.; Saraswat, B. S.; Mehrotra, R. C. *Polyhedron* **1985**, *4*, 2089–2096.